

UC Irvine

UC Irvine Previously Published Works

Title

Fluorescence lifetime distributions in proteins

Permalink

<https://escholarship.org/uc/item/3tq363xp>

Journal

Biophysical Journal, 51(4)

ISSN

0006-3495

Authors

Alcala, JR
Gratton, E
Prendergast, FG

Publication Date

1987-04-01

DOI

10.1016/s0006-3495(87)83384-2

Copyright Information

This work is made available under the terms of a Creative Commons Attribution License, available at <https://creativecommons.org/licenses/by/4.0/>

Peer reviewed

FLUORESCENCE LIFETIME DISTRIBUTIONS IN PROTEINS

J. RICARDO ALCALA,* ENRICO GRATTON,* AND FRANKLYN G. PRENDERGAST[†]

**Physics Department, University of Illinois at Urbana-Champaign, Urbana, Illinois 61801;*

[†]*Department of Biochemistry and Molecular Biology, Mayo Foundation, Rochester, Minnesota 55905*

ABSTRACT The fluorescence lifetime value of tryptophan residues varies by more than a factor of 100 in different proteins and is determined by several factors, which include solvent exposure and interactions with other elements of the protein matrix. Because of the variety of different elements that can alter the lifetime value and the sensitivity to the particular environment of the tryptophan residue, it is likely that non-unique lifetime values result in protein systems. The emission decay of most proteins can be satisfactorily described only using several exponential components. Here it is proposed that continuous lifetime distributions can better represent the observed decay. An approach based on protein dynamics is presented, which provides fluorescence lifetime distribution functions for single tryptophan residue proteins. First, lifetime distributions for proteins interconverting between two conformations, each characterized by a different lifetime value, are derived. The evolution of the lifetime values as a function of the interconversion rate is studied. In this case lifetime distributions can be obtained from a distribution of rates of interconversion between the two conformations. Second, the existence of a continuum of energy substates within a given conformation was considered. The occupation of a particular energy substate at a given temperature is proportional to the Boltzmann factor. The density of energy states of the potential well depends upon the width of the well, which determines the degree of freedom the residue can move in the conformational space. Lifetime distributions can be obtained by association of each energy substate with a different lifetime value and assuming that the average conformation can change as the energy of the substate is increased. Finally, lifetime distributions for proteins interconverting between two conformations, each characterized by a quasi-continuum of energy substates, are presented. The origin of negative components of the lifetime distribution is also discussed. In the companion paper that will follow (Alcala, J. R., E. Gratton, and F. J. Prendergast, 1987, *Biophys. J.*, in press) lifetime distributions obtained here are used to fit experimental data.

INTRODUCTION

The investigation of intrinsic fluorescence from proteins has been regarded as an effective method to study protein conformations and dynamics. The structural information is associated with the sensitivity of the emission spectrum of tryptophan and tyrosine residues to the nature of its environment. Dynamic information has been obtained from the analysis of the decay of the emission anisotropy and other excited state processes such as quenching by fast diffusing molecules or resonance energy transfer. Fluorescence lifetime measurements have instead been used to infer the existence of different and unique protein conformations (1). Conventionally, the decay is resolved in terms of exponential components, and the values of the decay rates and preexponential factors of each component are associated with a particular conformation and with the relative population of each conformation. However, the accurate study of the emission from several single tryptophan proteins has shown that the number of lifetime components can be large and that the identification with

different protein conformations can be difficult (2). The purpose of this work is to investigate the possibility that the complex decay observed for several proteins can reflect some aspects of protein structure and dynamics, which have been recently proposed as a unique property of protein systems (3). The existence of a large number of conformational substates and the dynamics of interconversion between substates can in principle be probed using fluorescence methodologies.

The sensitivity of indole fluorescence to a wide variety of environmental conditions is well recognized (4, 5) and is the principal factor in the diversity of fluorescence observed between different peptides and proteins, even when each of the proteins being studied contains a single tryptophan residue. Lifetime values can differ by more than a factor of 100 among different proteins (1). Solvation is certainly a major factor in determining the nature of tryptophan fluorescence, but there are many other moieties intrinsic to the protein structure and/or excited state processes that can affect the fluorescence lifetime markedly (6). Intramolecular groups likely to interact with tryptophan residues can quench the fluorescence. In a protein, dynamic quenching by groups intrinsic to the

Address correspondence to Dr. Gratton.

protein matrix will be determined by structural fluctuations occurring on the same time scale as the emission process and inevitably will involve nondiffusive motions of both the quenching agent and the indole ring of the tryptophan moiety itself. There are multiple factors that can affect the lifetime. Chemical moieties that can quench tryptophan fluorescence include ionic species (e.g., histidyl, carboxyl, or arginyl residues), disulfide bonds, methionyl sulfur or sulfhydryl groups, and carbonyl groups of peptide bonds (7). To quench, these moieties must be sufficiently close to allow "collisions" with the tryptophan ring. Protein-bound metal ions, especially paramagnetic species or metal ions that can form charge-transfer complexes, can also affect the lifetime markedly. Moreover, these interactions can occur through space, although the distance dependence of their effects are not known with certainty (8, 9). Some metal ions may also promote intersystem crossing to enhance phosphorescence at the expense of fluorescence, and there are other excited state processes, including excitation energy transfer and dipolar relaxation, that alter the decay of the excited state. Dipolar relaxation has not been demonstrated unequivocally as a factor influencing tryptophan fluorescence but is a possible participant (10). Lastly, we can surmise that torsional motions of the tryptophan ring can also influence the efficiency of the excitation and emissive processes. Ilich and Callis (manuscript submitted for publication) have recently shown that the indole ring is slightly puckered in the ground state but becomes planar in the excited state, which presumably reflects delocalization during the excited state of the lone pair of electrons on the nitrogen into the aromatic system. Distortions of indole ring planarity during the excited state, caused by mechanical factors associated with the dynamics of the protein matrix forming the tryptophan environs, are entirely possible and would be reflected in shortened lifetime values.

One basic assumption of this work is that quasi-continuous fluorescence lifetime distributions can arise in proteins since the decay rates are strongly dependent upon the local protein conformation and dynamics. For a given residue, the conformation of the protein characterizes its environment which determines, for example, the quenching mechanisms that affect its excited state lifetime. The dynamics determines the rates of interconversion among conformations. As such rates increase, e.g., as effected by an increase in temperature, the residue will experience a wider variety of environments during the excited state and, consequently, its lifetime will change.

In the following sections some mathematical models are presented that reflect the above ideas and give rise to continuous lifetime distributions. A physical justification for each model is also given based on the present knowledge of protein structure and dynamics. First, a two-states model is presented that can give only two well defined lifetime values. Continuous lifetime distributions can originate, in this picture, from a distribution of interconversion

rates between the two states. In this context this model is purely dynamic since the lifetime distribution is directly related to the dynamics of interconversion. Second, a quasi-continuum of energy substates within a single potential well is introduced. It is assumed that the substates are stable during the excited state lifetime. A quasi-continuum set of lifetime values is obtained in this model by association of each substate with a different decay rate. Last, lifetime distributions of two potential wells, each characterized by a quasi-continuum of substates that interconvert during the excited state lifetime, are considered.

TWO-STATE SYSTEM WITH DISTRIBUTED INTERCONVERSION RATES

Regarding Fig. 1, suppose the tryptophan residue can occupy two different positions in the protein molecule each characterized by a different value of the lifetime. This situation can occur due to the extreme sensitivity of the decay rate upon the local environment. For the interconverting and decaying two-state system of Fig. 1 *a*, states *a* and *b* are characterized by decay rates K_a and K_b , which

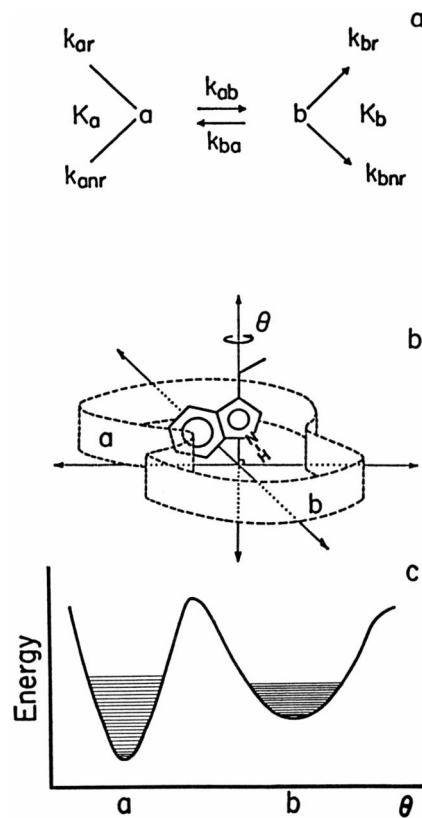


FIGURE 1 (a) Interconverting and decaying two state system. k_{ar} , k_{br} , k_{anr} , k_{bnr} , k_{ab} , and k_{ba} are the radiative decay, nonradiative decay, and interconverting rate constants, respectively, of states *a* and *b*. $K_a = k_{ar} + k_{anr}$ and $K_b = k_{br} + k_{bnr}$. (b) Schematic representation of a tryptophan residue in a protein. The energy of the residue is a function of the coordinate θ . (c) Relative potential energy surface in one dimension as a function of the conformational coordinate θ . Energy substates are represented by horizontal lines.

are the sum of the radiative (k_{ar} , k_{br}) and nonradiative (k_{anr} , k_{bnr}) decay rates of states a and b, respectively. The rates of interconversion between states a and b are k_{ab} and k_{ba} , respectively. A population of excited molecules distributes between the two states according to an equilibrium constant $H = k_{ab}/k_{ba}$. For free decay (without further excitation), the number (or fraction) of excited molecules in each state a and b can be described by the following first order coupled differential equations:

$$da/dt = -\Gamma_a a + k_{ba} b \quad (1a)$$

$$db/dt = k_{ab} a - \Gamma_b b \quad (1b)$$

with $\Gamma_a = k_{ab} + K_a$ and $\Gamma_b = k_{ba} + K_b$. The solution of the above system of equations is

$$a(t) = a_1 e^{-m_1 t} - a_2 e^{-m_2 t} \quad (2a)$$

$$b(t) = b_1 e^{-m_1 t} - b_2 e^{-m_2 t} \quad (2b)$$

where

$$m_{1,2} = 1/2[\Gamma_a + \Gamma_b \pm [(\Gamma_a - \Gamma_b)^2 + 4k_{ab}k_{ba}]^{1/2}] \quad (3)$$

$$a_1 = [a_0(\Gamma_a - m_2) - b_0 k_{ba}]/(m_1 - m_2) \quad (4a)$$

$$a_2 = [a_0(\Gamma_a - m_1) - b_0 k_{ba}]/(m_1 - m_2) \quad (4b)$$

$$b_1 = [b_0(\Gamma_b - m_2) - a_0 k_{ab}]/(m_1 - m_2) \quad (4c)$$

$$b_2 = [b_0(\Gamma_b - m_1) - a_0 k_{ab}]/(m_1 - m_2) \quad (4d)$$

The constants a_0 and b_0 are determined by the initial number (or fraction) of excited molecules in each state selected by the excitation and are therefore functions of the excitation wavelength. They can have any arbitrary positive value, which can lead to positive and negative preexponential factors. The fluorescence intensity at any given emission wavelength is then given by the radiative decay from a and b:

$$I_F(t) = Aa(t) + Bb(t). \quad (5)$$

The preexponential factors and the decay rates in Eq. 5 are functions of the four rate constants (K_a , K_b , k_{ab} , and k_{ba}) of Fig. 1 a. The constants A and B depend on the emission wavelength. The fluorescence decays as a double exponential but the characteristic rates m_1 and m_2 and the corresponding preexponential factors cannot be associated with molecules in state a or b, being the eigenvalues and eigenvectors of the entire system. Fig. 2, a–c shows the evolution of the preexponential factors, lifetimes, and average intensity (normalized to one) as a function of the interconversion time (inverse of the rates), respectively. For the calculations of Fig. 2 it was assumed that equal fractions of molecules in each conformation were excited at time zero. The equilibrium constant H was 2. The lifetimes of the states a and b were 1 and 10 ns, respectively. Two limits are worth mentioning here: (a) When the rates of interconversion are much faster than the decay rates, a

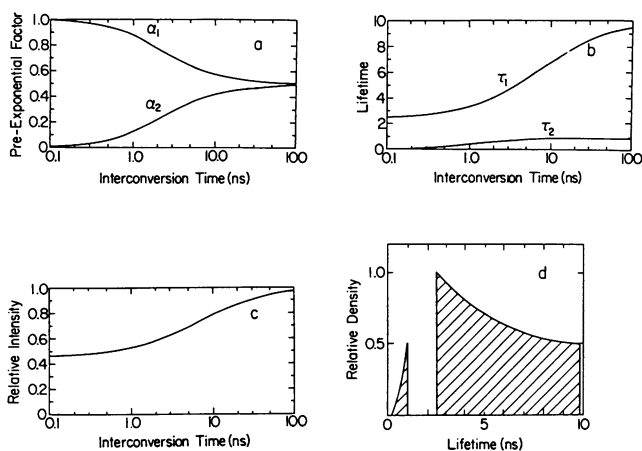


FIGURE 2 Evolution of a two-state fluorescent system as a function of the interconversion time between the two states. The equilibrium constant was 2. Equal fractions of molecules in each state were selected by the excitation. The lifetimes of the isolated states were 1 and 10 ns. Evolution of (a) preexponential factors, (b) lifetime values, (c) average intensity as a function of the interconversion times. (d) Lifetime distribution from a uniform distribution of activation energies for the system in a–c.

single exponential decay is observed. In this case, the longer lifetime component has the larger value of the preexponential factor and the decay rate is given by the following equation:

$$K = (K_a + H * K_b)/(H + 1). \quad (6)$$

(b) When the rates of interconversion are much slower than the decay rates, molecules in states a and b decay like two independent components with unique decay constants, which are the characteristic decay rates of each state.

For the two-state system the following general conclusions can be stated. (a) Only two decay rates characterize the decay; (b) For constant radiative and nonradiative decay rates of the individual states, the average intensity observed or equivalently, the apparent quantum yield of an interconverting system, decreases when its dynamics speed up (Fig. 2 c).

Distributions of interconversion rates among substates have been proposed for proteins (11). Such distributions of rates arise from the multiplicity of substates of a protein. The potential energy barrier heights, which in our case separate the two states and determine the value of k_{ab} and k_{ba} , can be different for each protein molecule. Fig. 2 d shows a distribution of lifetimes obtained under the circumstances established above. It is assumed that these rates can be described by the relationship $k = k_0 e^{-E/T}$ where E is the activation energy uniformly distributed in the range $0-6.9T$ and k_0 was set to 10^{10} s^{-1} (energy is measured in units of temperature). If other distribution functions are used, different shapes for the lifetime distribution can be obtained. The particular form for the activation energy distribution to be used can be determined experimentally. For the two-state system a bimodal life-

time distribution is obtained since two average lifetimes are characteristic of the system.

DISTRIBUTION OF SUBSTATES IN A POTENTIAL WELL

The two-state system discussed in the previous section with distributed energy barriers represent one possibility for producing distributions of rates. In this section we analyze the case in which the characteristic decay rate of one individual conformation is described by a distribution. Consider the case illustrated in Fig. 1 *b* in which the position of the indole ring in a protein pocket is determined by the angle θ around which the ring rotates about the carbon-carbon axis. Most of the quenching mechanisms are a function of the distance, orientation, etc., between the indole ring and the quenching agent, and a quasi-continuous set of decay rates can be generated as a function of the angle θ . In essence, we are now considering a quasi-continuous set of configurations rather than two conformations, as we did in the previous section. For the purpose of what follows we redefine the concept of conformation as a potential well with a multitude of energy substates. Fig. 1 *c* shows two conformations corresponding to states a and b of the previous section separated by a potential energy barrier. The energy substates must not be confused with the conformational substates introduced by Frauenfelder and co-workers (11). Different energy substates can have the same average configuration. The total energy of the residue distributes between kinetic (dynamic) and potential (conformational). The residue will adopt preferentially the values of the conformational coordinate θ , which minimize the overall potential energy of the protein. To derive an expression for the fluorescence decay of this system, the number of energy substates, the occupation of each substate, and the decay rate from each substate must be determined.

Residues distribute in the energy substates according to the Boltzmann factor.

$$P(\epsilon) = e^{-\epsilon/T}. \quad (7)$$

The fraction of residues in a given conformation with energies larger than the potential barriers that define the well a in Fig. 1 *c*, can shift to the adjacent conformation b. For the derivations of this section no interconversion between wells is considered; instead interconversion between potential wells is treated in the next section. The degree of flexibility in a given conformation is determined by the width of the potential well. Wider wells allow larger fluctuations around the average conformation than do narrower wells. Consequently, a residue in a wide potential well is exposed to a larger variety of environments with respect to a residue in a narrow well and its lifetime distribution should be sensitive to the well width. In terms of the model presented in this section, the configuration and occupancy of energy substates remain invariant during the excited state lifetime.

Potential wells are characterized by their density of states $D(\epsilon)$, which increase with the width of the well. A functional form for the density of states, which is frequently used for several quantum and semi-classical systems, is given by

$$D(\epsilon) = \text{const}' (\epsilon + \epsilon_0)^\beta \quad \beta < 0 \quad (8)$$

$$D(\epsilon) = \text{const} (\epsilon - \epsilon_0)^\beta \quad \beta > 0. \quad (9)$$

The parameter β , which characterizes the width of the well and the density of states, is related to the microenvironment of the excited residues. For example, a smaller value of β could represent a residue with a very restricted motional freedom. Alternatively, a relatively large value of β could represent a residue with high freedom to move, exposed to the solvent and to a large variety of protein environments.

The fluorescence is the sum over all radiative contributions from each excited residue

$$I_F(t) = \int_{\epsilon_0}^{\infty} P(\epsilon) D(\epsilon) \int_{\theta} I_s(\theta, \epsilon, t) d\theta d\epsilon, \quad (10)$$

where $I_s(\theta, \epsilon, t)$ is the fluorescence from the protein residue in conformational coordinate θ . Each value of θ has a different decay rate, which implies a single exponential decay for each conformational coordinate. The limits of integration include all possible energies and conformations. The absolute value of the lowest energy state, ϵ_0 , throughout the present discussion has been assumed small. Therefore from Eq. 10, the fluorescence from each potential well is given by a continuous distribution of exponential decays, and the lifetimes and amplitudes are a function of the conformational coordinate, the energy of the system, and potential well shape. Eq. 10 can be rewritten in the following form:

$$I_F(t) = \int_{\epsilon_0}^{\infty} P(\epsilon) D(\epsilon) I_w(\epsilon, t) d\epsilon, \quad (11)$$

where $I_w(\epsilon, t)$ is the fluorescence intensity of the energy state ϵ averaged over all conformational coordinates. The distribution of rates, which arise from different conformational coordinates within an energy state, is characterized by a gaussian centered at $k(\epsilon)$ and of relatively narrow width such that it can be substituted by an average value given by an exponential

$$I_w(\epsilon, t) = k_r e^{-k(\epsilon)t}, \quad (12)$$

where $k(\epsilon)$ is the average decay rate of the state of energy ϵ and k_r is the natural (radiative) decay rate. In what follows, the radiative decay of the tryptophan residue has been assumed constant and independent on the particular protein conformation and dynamics. It depends mainly upon the electronic structure of the residue and can be determined using the equation of Strickler and Berg (12). This assumption is valid provided no major changes in the index of refraction or in the overall integrated absorption

spectrum take place with fluctuations around the average conformation. The absorption spectrum of tryptophan is largely insensitive to solvent. For a wide variety of proteins the natural (radiative) lifetimes of tryptophan residues obtained from the absorption spectrum yielded comparable values (13), which supports the invariance of the radiative decay rate with conformation and dynamics.

One of the assumptions inherent in the model we are analyzing is that the decay rate is determined by the value of the conformational coordinate θ . To obtain a relationship between energy and decay rate we now assume that, as the energy of the substate increases, the average conformational coordinate also changes, which implies that the potential well is asymmetric. We express the relationship between the average nonradiative decay rate and the substate energy using the equation

$$k_{nr} = B(T) + C(1 - e^{-\epsilon/T}), \quad (13)$$

which was consistent with the data fits reported in the companion paper (13a) and we justify as follows. The low energy states are practically frozen conformations at the bottom of the well, and their nonradiative decays are given by the conformational coordinate dependent rate constant $B(T)$, which also contains the temperature dependence of the nonradiative decay rate. As the energy of the residue increases it samples a larger number of microenvironments. The limiting decay rate for the highest energy substate is given by the asymptotic, well-dependent value of Eq. 13, $B(T) + C$, where C is a constant that depends on the asymmetry of the potential well. For a symmetric potential well $C = 0$. Eq. 13 is consistent with Fig. 2c (when C is positive), which shows that the average intensity varies between the two limits determined when the rates of interconversion are much slower and much faster than the decay rates, respectively.

The average overall fluorescence decay rate as a function of the energy can then be expressed by the expression

$$k(\epsilon) = A(T) + C(1 - e^{-\epsilon/T}), \quad (14)$$

where $A(T) = k_r + B(T)$, and the observed fluorescence can be written in the following form

$$I_F(t) = \int_{\epsilon_0}^{\infty} P(\epsilon)D(\epsilon)Q(\epsilon)k(\epsilon)e^{-k(\epsilon)t} d\epsilon, \quad (15)$$

where $P(\epsilon)$, $D(\epsilon)$, and $k(\epsilon)$ have previously been defined. $Q(\epsilon)$ is the quantum yield given by the ratio of the radiative to the total decay rate. Using Eq. 14 the variable of integration in Eq. 15 can be changed to decay rates. Furthermore, the lifetime is the inverse of the decay rate and the integration can be conducted in lifetime space to obtain the following results:

$$I_F(t) = \int_{\tau_L}^{\tau_0} n(\tau)\tau^{-1}e^{-t/\tau} d\tau, \quad (16)$$

where

$$n(\tau) = N\tau^{-1}\{\ln[\tau(\tau_0 - \tau_L)/\tau_0(\tau - \tau_L)]\}^\beta \quad (17a)$$

$$\tau_0 = A(T)^{-1} \quad (17b)$$

$$\tau_L = [A(T) + C]^{-1}, \quad (17c)$$

subject to the following normalization condition (to determine the constant N)

$$\int_{\tau_L}^{\tau_0} n(\tau) d\tau = 1. \quad (18)$$

τ_0 is the maximum lifetime at a given temperature and τ_L is the minimum lifetime, which is related to the asymmetry of the potential well. Fig. 3, *a-e* shows the variation of the lifetime distribution function defined by Eq. 17a as the width of the potential well increases. The maximum and minimum lifetimes (τ_0 and τ_L) used for the simulations of Fig. 3 were 5 and 0.5 ns, which are typical extremes of fluorescence lifetimes of tryptophan residues in proteins. Fig. 3, *a-e* was generated from Eq. 17a convoluted with a gaussian distribution, which represents the average lifetime at a given energy ϵ as previously discussed. The width

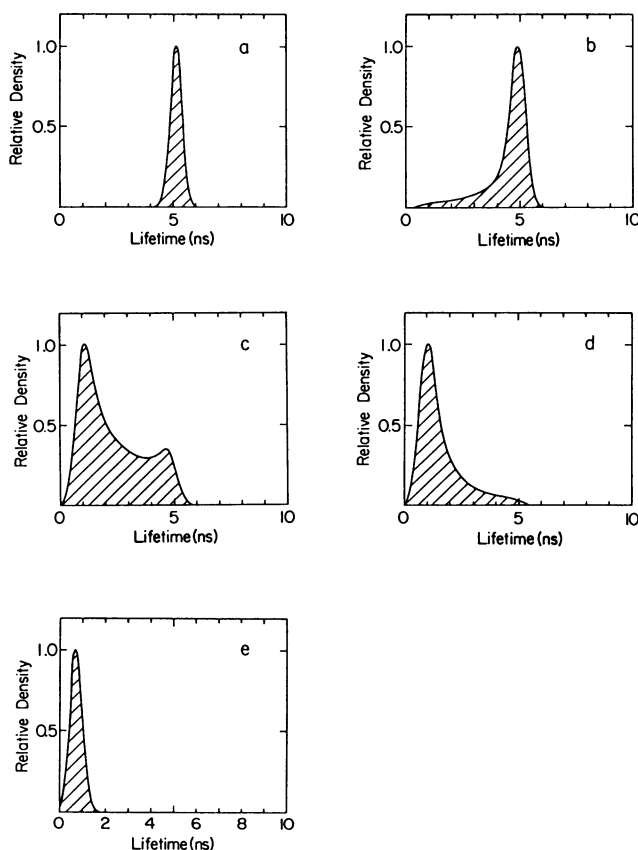


FIGURE 3 Evolution of the single potential well distribution as a function of the density of states of the excited residue in a protein. (a) Only one state which can correspond to a single environment for the residue. (b-e) The density of states increase monotonically, which causes larger fractions of the excited population of molecules to decay with shorter lifetimes. The values of β from *a* to *e* are -5 , -1 , 0 , 1 , and 5 .

of the gaussian was 0.5 ns (which is beyond the resolvability limit [14] of ~ 1 ns of the data provided by current instrumentation [15]). In Fig. 3 *a* the power of the density of states is -5 , which implies a very narrow potential well. Practically only one state (the ground state) is occupied. In this case, the distribution function yields an average single exponential decay (narrow gaussian distribution). As the density of states increases a larger fraction of residues occupies states other than the ground state. Additionally the average conformational coordinate of the higher energy substates is different from that of the lower energy substates due to the asymmetry of the potential well. Consequently, the lifetime distribution will depart from the single exponential. Shorter components start to appear in Fig. 3 *b* and their fraction increases with the availability of states and environments. This fact is consistent with the discussion presented in the previous section, which concluded that the larger the number of microenvironments and the faster the interconversion rate, the shorter the average lifetime observed. In Fig. 3 *c* the distribution changes skewness from the original right to left. Finally in Fig. 3 *e* ($\beta = 5$) a narrow distribution with a center at a short lifetime value is reached. In this latter case the large availability of states even at lower energies causes the protein residue to experience a wide variety of environments during the excited state lifetime, and a narrow distribution is observed. The limit obtained in Fig. 3 *e* is analogous to the single exponential limit obtained in the case of the two-state system when the rate of interconversion was much faster than the fluorescence decay rate. Such a situation might be observed experimentally in proteins with a high degree of freedom of the tryptophan residue at sufficiently high temperatures. When the excited residue can exist in more than one potential well the fluorescence lifetime distribution becomes sensitive to the interconversion among different conformations, as discussed in the following section.

THE DOUBLE POTENTIAL WELL LIFETIME DISTRIBUTION

The fluorescence intensity is determined by the radiative contributions from the decays of the excited residues in each potential well

$$I_F(t) = I_{Fa}(t) + I_{Fb}(t), \quad (19)$$

where $I_{Fa}(t)$ and $I_{Fb}(t)$ represent the fluorescence emitted from each conformation as a function of time and are given by Eq. 15. In this section it was assumed that the processes of interconversion are adiabatic and that all energy states interconvert with the same average constant rate. Similarly, as in the first section of this paper, the two limiting behaviors are (*a*) when the rates of interconversion are much slower than the decay rates the lifetime distribution becomes the superposition of the two independent single potential well distributions, and (*b*) when the rates of

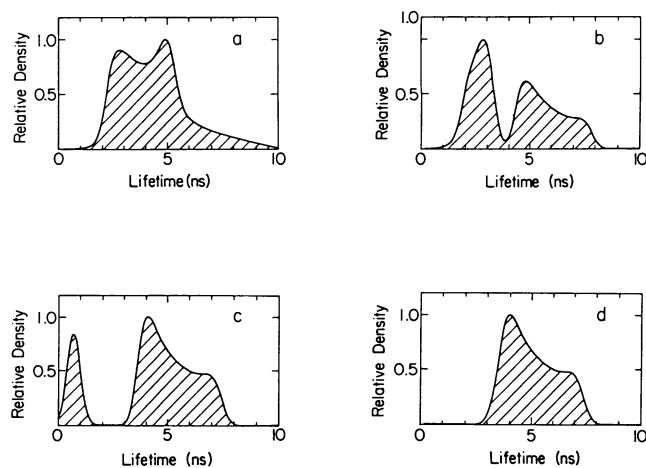


FIGURE 4 Evolution of a two potential well distribution with excitation at conformational equilibrium. The value of the conformational equilibrium constant was 2. $2/3$ of the residues were excited in the shorter lived conformation. The lifetime distributions of the two conformations spread in adjacent lifetime intervals. The longer lived conformation extends in the $\tau_L = 6$ ns to $\tau_O = 9$ ns range and the shorter lived conformation extends in the $\tau_L = 2$ ns to $\tau_O = 5$ ns lifetime interval. The interconversion times in *a-d* are 100, 10, 1, and 0.1 ns, respectively. The values of β for the density of states functions were -0.4 and -0.6 , respectively.

interconversion are much faster than the decay rates the lifetime distribution is given by an effective single potential well. The two potential well lifetime distribution yielded expressions highly complex and are not presented here. In Figs. 4 and 5 the evolution of two potential well lifetime distributions as a function of the interconversion rates is shown for excitation at equilibrium and far from equilibrium, respectively.

The excitation photoselects the residues according to their environment. Once excited, the selected population interconverts between the two conformations during the lifetimes. If the rates of interconversion are much faster

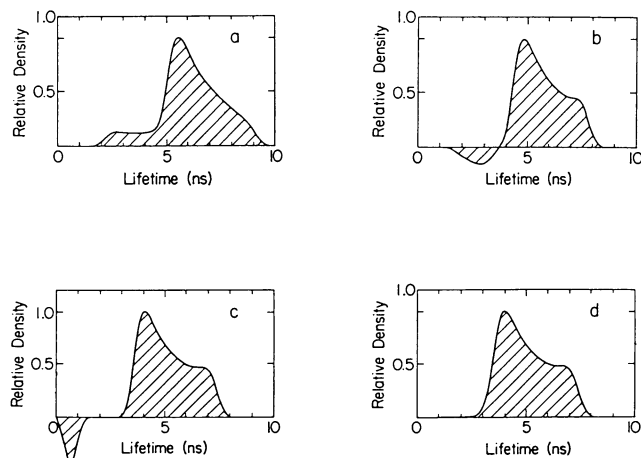


FIGURE 5 Evolution of the two potential well distribution with selective excitation of the population of residues far from equilibrium. The parameters used are those of Fig. 4. At time zero 90% of the excited molecules are in the longer lived conformation.

than the decay rates, the excited population of residues reaches the conformational equilibrium before decaying. If the rates of interconversion are much slower than the rates of decay, then the two conformations decay independently. Finally, when both the decay rates and the interconversion rates are of the same order of magnitude, a drift of the excited population to the conformational equilibrium takes place during the fluorescence decay. The fluorescence lifetime distribution is highly dependent upon the rates of interconversion and upon the excitation as discussed below. In Fig. 4 the evolution, with increasing interconversion rates, of the lifetime distribution selectively excited in conformational equilibrium is shown (the value of the conformational equilibrium constant was 2). The most populated conformation in equilibrium was the shorter lived. Consequently, 2/3 of the residues were excited in the shorter lived conformation. The lifetime distributions of the two individual conformations spread in adjacent lifetime intervals. For the simulations of Figs. 4 and 5, the longer lived conformation extended in the 6–9-ns range, and the shorter lived conformation was in the 2–5-ns lifetime interval. In Fig. 4 *a* the interconversion time from the longer lived well to the shorter lived well τ_{ab} ($= 1/k_{ab}$) was 100 ns. In this case the rates of interconversion are about an order of magnitude slower than the decay rates. This situation may correspond to a low temperature decay in which the two conformations can be regarded as frozen. The distribution obtained was quite broad and most of the fluorescence decays with relative shorter lifetimes. Fig. 4 *d* shows the effective single potential well limit when the rates of interconversion are much faster than the decay rates ($\tau_{ab} = 0.1$ ns). The lifetime distribution was narrower than the frozen distribution. Fig. 4, *b* and *c* shows intermediate distribution shapes for interconversion rates of comparable orders of magnitude with the decay rates ($\tau_{ab} = 10$ ns and 1 ns, respectively). The two parts of the distribution in Eq. 19 which were broad, adjacent, and shifted to longer lifetimes in the frozen limit become narrower, distinguishable, and shifted to shorter lifetimes with increasing interconversion rates. It should be mentioned that except for the frozen limit such distributions do not represent the lifetimes of the independent conformations. In Fig. 5 we show the evolution of negative amplitude lifetime distributions due to selective excitation of the population of residues far from equilibrium. The rates are the same as in Fig. 4 but the initial conditions were different. In this case 90% of the molecules are excited in the longer lived conformation. In Fig. 5 *a* the interconversion time from the longer lived well to the shorter lived well, τ_{ab} , was 100 ns. In this case the rates of interconversion are about an order of magnitude slower than the decay rates. This situation again may correspond to a lower temperature decay in which the two conformations can be regarded as frozen. The distribution was quite broad and most of the fluorescence decays with relative long lifetimes. As the rates of interconversion speeded up, the distribution

became narrower and shifted to shorter lifetimes. In Fig. 5 *b*, τ_{ab} is 10 ns. Negative components (preexponential factors) start to appear, which is an indication of the conformational drift to equilibrium during the fluorescence decay. The shifting to equilibrium occurs more efficiently during the decay time interval as the rate of interconversion increased. For $\tau_{ab} = 1$ ns, in Fig. 5 *c*, the negative amplitudes increase. It should be mentioned that the negative amplitudes appear in the shorter lifetime interval due to the choice of the initial conditions for which the longer lived conformation populates the shorter lived. For faster interconversion rates, the negative amplitudes start to decrease and finally, as shown in Fig. 5 *d*, for an interconversion time of $\tau_{ab} = 0.1$ ns (and shorter), the excited population reaches the conformational equilibrium in much shorter times than the lifetime. In this situation the shape of the observable lifetime distribution was independent of the initial excited population, as can be seen by comparison of Figs. 4 *d* and 5 *d* in which initial conditions were very different. The evolution of the lifetime distribution with temperature can be analogous to the cases shown in Figs. 4 and 5. However, in these figures the equilibrium constant $H = 2$ was fixed. The variation of such interconversion equilibrium constant with temperature will have to be taken into consideration to study the evolution of the lifetime distribution with temperature.

CONCLUSIONS

In the case of an interconverting system the lifetime values obtained from either discrete or distributed models constitute apparent values that do not represent the real lifetimes of the conformations. This fact can be seen throughout the discussions of both interconverting models in which the decay rates are shown to be functions of both conformation and dynamics of the system. Similarly, the preexponential factors cannot be related to the fraction (or number) of molecules in each conformation. Only in the frozen limit (negligible interconversion rates) do the discrete and distributed fluorescence lifetimes obtained yield the real decay times of the system. Additionally, in such limit the preexponential factors (discrete or distributed) are sensitive to the population selected by the excitation. The discussion of the two potential well system with distributed barriers and distributed decay rates from each conformation can be generalized to a multi-potential well case. The overall distribution obtained will be the superposition of a variety of distributions in which negative and positive amplitudes superimpose. In this case the distribution can be complex and the study of individual or limited components of the distribution obtained is suggested.

We propose that the fluorescence decay of a protein system can be analyzed in terms of multiple interconverting conformations. Hypotheses regarding the nature of the system can be tested, such as the variation of the conformational equilibrium constants with temperature, the popula-

tion selected by the excitation, the relations between energy state and decay rate, and so on. These hypotheses, when included in the fitting process, reduce the number of degrees of freedom and require global analysis of large sets of data (16). From this point of view, the practice of inverting the Laplace transform (17, 18) to study the decay of the population (even if perfect data were available) will yield the overall lifetime distribution but will provide little information with regard to the functional form of the distribution which instead contains the physics of the system.

The relative potential energy as a function of the conformational coordinates currently proposed for proteins (19, 20) assumes a large variety of minima. These minima are usually regarded as relative stable conformations of the protein (at low enough temperature). As the protein travels through conformational space it encounters the potential wells in a defined order. In this manner, the potential energy surface in conformational space defines not only the stable conformations but also determines the hierarchical pattern for protein fluctuations. It is important to note that fluorescence processes are most sensitive to events in the immediate vicinity of the excited residue. Moreover, the excited state dynamics and hierarchy of such localized regions of the protein may be different from its ground state, inasmuch as the excited dipoles may locally modify the structure and dynamics of its environs. In the derivation of lifetime distributions the behavior of the excited state was assumed with no relation to the ground state mechanics. In the companion paper that will follow (13a) some lifetime distributions obtained here are used to fit experimental data. The results are discussed in terms of the environment of the tryptophan residue in the proteins.

We would like to thank Dr. J. P. Palmeri for his suggestions regarding the development of the single potential well model. We would also like to acknowledge Dr. H. Frauenfelder for the fruitful discussions that influenced the concepts presented here and J. Beechem for his suggestions concerning the preparation of the manuscript.

Financial support for this work was provided by a grant from a National Science Foundation (grant PCM 84-03107) a NAVAIR grant MDA 903-85-X-0027 to E. Gratton and J. R. Alcalá, and Public Health Service grant GM-34847 to F. G. Prendergast.

Received for publication 20 August 1986 and in final form 16 December 1986.

REFERENCES

1. Beechem, J., and L. Brand. 1985. Time resolved fluorescence decay in proteins. *Annu. Rev. Biochem.* 54:43-71.
2. Gratton, E., J. R. Alcalá, G. Marriott, and F. G. Prendergast. 1986. Fluorescence studies of protein dynamics. Proceedings of the

- International Symposium on Computer Analysis for Life Science. Hayashibara Forum '85. C. Kawabata and A. R. Bishop, editors. Ohmsha, Ltd., Okayama, Japan. 1-11.
3. Ansari, A., J. Berendzen, S. F. Bowne, H. Frauenfelder, I. E. T. Iben, T. B. Sauke, E. Shyamsunder, and R. D. Young. 1985. Protein states and proteinquakes. *Proc. Natl. Acad. Sci. USA.* 82:5000-5004.
4. Creed, D. 1984. The photophysics and photochemistry of the near-UV absorbing amino acids-I. Tryptophan and its simple derivatives. *Photochem. Photobiol.* 39:537-562.
5. Creed, D. 1984. The photophysics and photochemistry of the near-UV absorbing amino acids-II. Tyrosine and its simple derivatives. *Photochem. Photobiol.* 39:563-575.
6. Lumry, R., and M. Hershberger. 1978. Status of indole photochemistry with special reference to biological applications. *Photochem. Photobiol.* 27:819-840.
7. Longworth, J. W. 1971. Luminescence of polypeptides and proteins. *In Excited States of Proteins and Nucleic Acids.* R. F. Steiner and I. Weinryb, editors. Plenum Publishing Corp., New York. 319-484.
8. Chen, R. F. 1976. The effect of metal cations on intrinsic protein fluorescence. *In Biochemical Fluorescence.* Vol. 2. R. F. Chen and H. Hedelhoc, editors. Marcel Dekker, Inc., New York. 573-606.
9. Engel, L. W., and F. G. Prendergast. 1987. Sensitized indole to terbium energy transfer in n-indole/EDTA/terbium complex studied by use of luminescence quenching. *Biochemistry.* 25:831-834.
10. Lakowicz, J. R., and H. Cherek. 1980. Dipolar relaxation in proteins on nanosecond timescale observed by wavelength-resolved phase fluorometry of tryptophan fluorescence. *J. Biol. Chem.* 831-834.
11. Austin, R. H., K. W. Beeson, L. Eisenstein, H. Frauenfelder, and I. C. Gunsalus. 1975. Dynamics of ligand binding to myoglobin. *Biochemistry.* 14:5355-5373.
12. Strickler, S. J., and R. A. Berg. 1962. Relation between absorption intensity and fluorescence lifetimes of molecules. *J. Chem. Phys.* 37:814-822.
13. Fasman, G. D. 1975. *CRC Handbook of Biochemistry and Molecular Biology.* 3rd ed. Vol. II. CRC Press, Cleveland. 383-545.
- 13a. Alcalá, J. R., E. Gratton, and F. J. Prendergast. 1987. Fluorescence lifetime distributions in proteins by use of multifrequency phase fluorometry. *Biophys. J.* In press.
14. Alcalá, J. R., E. Gratton, and F. G. Prendergast. 1987. Resolvability of fluorescence lifetime distributions using phase fluorometry. *Biophys. J.* 51:587-596.
15. Alcalá, J. R., E. Gratton, and D. M. Jameson. 1985. A multifrequency phase fluorometer using the harmonic content of a mode-locked laser. *Anal. Instrum.* 14:225-250.
16. Beechem, J. M., M. Ameloot, and L. Brand. 1985. Global analysis of fluorescence decay surfaces: excited state reactions. *Chem. Phys. Lett.* 120:466-472.
17. Provencher, S. W. 1979. Inverse problems in polymer characterization: direct analysis of polydispersity with photon correlation spectroscopy. *Makromol. Chem.* 180:201-209.
18. Provencher, S. W., J. Hendrix, L. DeMaeyer, and N. Paulussen. 1978. Direct determination of molecular weight distributions of polystyrene in cyclohexane with photon correlation spectroscopy. *J. Chem. Phys.* 69(9):4273-4276.
19. Karplus, M., and J. A. McCammon 1983. Dynamics of proteins, elements and function. *Annu. Rev. Biochem.* 53:263-300.
20. Frauenfelder, H., and E. Gratton. 1985. Proteins dynamics and hydration. *Biomembranes, protons and water: structure and translocation.* *Methods Enzymol.* 127:471-492.